CANUM, 13-17 June 2022

DE LA RECHERCHE À L'INDUSTRIE

# Virtual element method for solving boundary integral equations of electro-magnetic scattering at a perfectly conducting body

Alexis Touzalin, Emanuele Arcese | CEA, Le Barp, France
Sébastien Pernet | ONERA, Toulouse, France

**Context**: Analysis of electromagnetic (EM) scattering phenomena by a complex object that

- can be electrically large (wrt. the wavelength), and
- often consists of multiple components of disparate sizes.

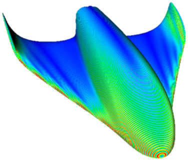

Figure: Example of EM scattering simulation of a Virgin-Galactic-like object.

**Motivation**: Accurate evaluation of Radar Cross Sections (RCS) using the boundary integral method.

**Difficulty**: Flexibility in generating an efficient mesh of the computational domain.

$\Rightarrow$ high CPU cost and memory footprint,

$\Rightarrow$ low quality of numerical solutions.

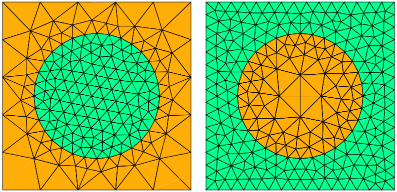

Figure: Examples of a conforming mesh of a square case containing a circle.

**Context**: Analysis of electromagnetic (EM) scattering phenomena by a complex object that

- can be electrically large (wrt. the wavelength), and
- often consists of multiple components of disparate sizes.

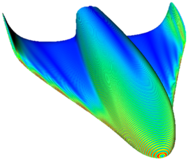

Figure: Example of EM scattering simulation of a Virgin-Galactic-like object.

**Motivation**: Accurate evaluation of Radar Cross Sections (RCS) using the boundary integral method.

**Difficulty**: Flexibility in generating an efficient mesh of the computational domain.

X Classical finite element methods (FEM) are well-established and adapted to HPC, ... but are not robust to element distortions and hanging nodes.

X Discontinuous Galerkin methods are good candidates, ... but at the cost of a significant increase in size of the linear system and in complexity of the weak formulation (due to the additional, e.g., penalty terms)

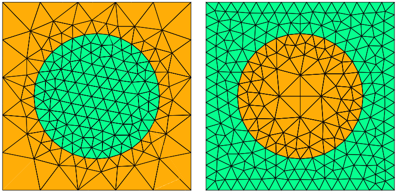

Figure: Examples of a conforming mesh of a square case containing a circle.

**Context**: Analysis of electromagnetic (EM) scattering phenomena by a complex object that

- can be electrically large (wrt. the wavelength), and
- often consists of multiple components of disparate sizes.

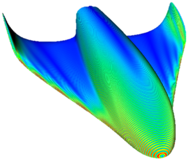

Figure: Example of EM scattering simulation of a Virgin-Galactic-like object.

**Motivation**: Accurate evaluation of Radar Cross Sections (RCS) using the boundary integral method.

**Objective**: Application of the recent Virtual Element Method (VEM) to boundary integral formulations in order to

⇒ simplify the gluing/adaptation of the existing classical (triangle) meshes,

⇒ improve the performance of the existing in-house FEM codes.

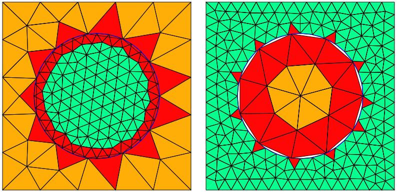

Figure: Examples of a nonconforming mesh of a square case containing a circle.

## 1 Presentation of the model problem

- Overview of frequency-domain Maxwell's equations of EM scattering
- Presentation of the weak formulation of the Electric Field Integral Equation (EFIE)

## 2 Discretization of the model problem

- Recall of the standard $H_{div}$-finite elements for solving the EFIE problem
- Application of VEM to the EFIE problem

## 3 Preliminary numerical results

- Analysis of two 3D test cases and discussion

**Presentation of the model problem**

**Maxwell's equations in frequency domain (notation: $e^{-\iota\omega t}$)**

$$
(1)\quad
\begin{cases}
\mathbf{curl}\boldsymbol{E} - \iota\kappa\mu\boldsymbol{H} = 0, \\
\mathbf{curl}\boldsymbol{H} + \iota\kappa\varepsilon\boldsymbol{E} = 0,
\end{cases}
\quad \text{in } \mathbb{R}^3 \setminus \bar{\Omega},
$$

$$
\begin{cases}
\boldsymbol{E} \times \boldsymbol{n} = 0, & \text{on } \Gamma := \partial\Omega, \\
RC(\boldsymbol{E} - \boldsymbol{E}^I,\ \boldsymbol{H} - \boldsymbol{H}^I) & \text{at infinity.}
\end{cases}
$$

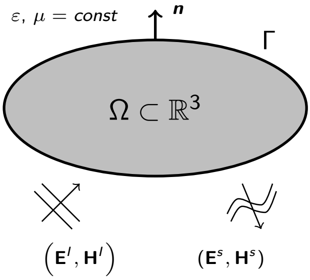


- total fields: $\boldsymbol{E}(\boldsymbol{x}) = \boldsymbol{E}^s(\boldsymbol{x}) + \boldsymbol{E}^I(\boldsymbol{x})$, $\boldsymbol{H}(\boldsymbol{x}) = \boldsymbol{H}^s(\boldsymbol{x}) + \boldsymbol{H}^I(\boldsymbol{x})$;
- $\varepsilon,\ \mu \in \mathrm{L}^\infty\left(\mathbb{R}^3 \setminus \bar{\Omega}\right)$;
- wave number and impedance in vacuum: $\kappa = \omega\sqrt{\varepsilon_0\mu_0}$; $\eta_0 = \sqrt{\mu_0/\varepsilon_0}$ with $\omega = 2\pi f$ and $f$ being the wave freq;
- with $RC(\boldsymbol{E} - \boldsymbol{E}^I,\ \boldsymbol{H} - \boldsymbol{H}^I)$ being the Silver-Müller radiation condition;
- N.B. : the magnetic field is scaled s.t. $\boldsymbol{H} = \eta_0\hat{\boldsymbol{H}}$.

# Some formulas of Integral Representation (IR)

Considering the homogeneous problem associated to (1), as sketched out below.
Let $\boldsymbol{J} = (\boldsymbol{n} \times \boldsymbol{H})|_\Gamma$ be the electric current tangential to $\Gamma$.
A solution $(\boldsymbol{E}, \boldsymbol{H})$ to (1) in $\Omega^+$ admits an IR via the Stratton-Chu formula:

$$\boldsymbol{E}^I(\boldsymbol{x}) + \iota\kappa\mathcal{R}_\kappa \boldsymbol{J}(\boldsymbol{x}) = \begin{cases} \boldsymbol{E}(\boldsymbol{x}), & \forall \boldsymbol{x} \in \Omega^+, \\ 0, & \forall \boldsymbol{x} \in \Omega^-, \end{cases}$$

$$\boldsymbol{H}^I(\boldsymbol{x}) + \mathcal{Q}_\kappa \boldsymbol{J}(\boldsymbol{x}) = \begin{cases} \boldsymbol{H}(\boldsymbol{x}), & \forall \boldsymbol{x} \in \Omega^+, \\ 0, & \forall \boldsymbol{x} \in \Omega^-. \end{cases}$$

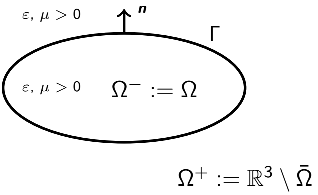


**where Maxwell (single- and double-layer) potentials and the Green kernel read**

$$\mathcal{R}_\kappa \boldsymbol{J}(\boldsymbol{x}) = \mu \int_\Gamma G_\kappa(\boldsymbol{x}-\boldsymbol{y})\boldsymbol{J}(\boldsymbol{y})\, d\gamma(\boldsymbol{y}) + \frac{1}{\kappa^2\varepsilon}\mathbf{grad}\int_\Gamma G_\kappa(\boldsymbol{x}-\boldsymbol{y})\,\mathrm{div}_\Gamma \boldsymbol{J}(\boldsymbol{y})\, d\gamma(\boldsymbol{y}), \quad \forall \boldsymbol{x} \notin \Gamma,$$

$$\mathcal{Q}_\kappa \boldsymbol{J}(\boldsymbol{x}) = \int_\Gamma \nabla_{\boldsymbol{x}} G_\kappa(\boldsymbol{x}-\boldsymbol{y}) \times \boldsymbol{J}(\boldsymbol{y})\, d\gamma(\boldsymbol{y}), \quad \forall \boldsymbol{x} \notin \Gamma,$$

$$G_\kappa(\boldsymbol{x}-\boldsymbol{y}) = \frac{e^{\iota\kappa|\boldsymbol{x}-\boldsymbol{y}|}}{4\pi|\boldsymbol{x}-\boldsymbol{y}|}, \quad \boldsymbol{x} \neq \boldsymbol{y}.$$

## The variational formulation of the Electric Field Integral Equation (EFIE) [1]

Find $\boldsymbol{J} \in H_{div}^{-1/2}(\Gamma)$, such that, provided $\kappa > 0$, and $\varepsilon, \mu > 0$ :

(2) $$a(\boldsymbol{J}, \boldsymbol{J}') = \frac{\iota}{\kappa} \int_\Gamma \boldsymbol{E}^I(\boldsymbol{x}) \cdot \boldsymbol{J}'(\boldsymbol{x})\, d\gamma(\boldsymbol{x}), \quad \forall \boldsymbol{J}' \in H_{div}^{-1/2}(\Gamma),$$

where

- $H_{div}^{-1/2}(\Gamma) = \left\{ \boldsymbol{v} \in H^{-1/2}(\Gamma, \mathbb{C}^3) \,|\, \boldsymbol{n} \cdot \boldsymbol{v} = 0 \text{ a.e. on } \Gamma, \quad \mathrm{div}_\Gamma \boldsymbol{v} \in H^{-1/2}(\Gamma) \right\}$,
- $a(\cdot,\cdot) : H_{div}^{-1/2}(\Gamma) \times H_{div}^{-1/2}(\Gamma) \to \mathbb{C}$ is the bilinear form associated with the tangential component of $\mathcal{R}_\kappa$, s.t.

$$(\boldsymbol{J}, \boldsymbol{J}') \mapsto \underbrace{\mu \int_{\Gamma\times\Gamma} G_\kappa(\boldsymbol{x}-\boldsymbol{y})\, \boldsymbol{J}(\boldsymbol{y}) \cdot \boldsymbol{J}'(\boldsymbol{x})\, d\gamma_y d\gamma_x}_{a_1(\boldsymbol{J},\boldsymbol{J}')} - \underbrace{\frac{1}{\kappa^2 \varepsilon} \int_{\Gamma\times\Gamma} G_\kappa(\boldsymbol{x}-\boldsymbol{y})\, \mathrm{div}_\Gamma \boldsymbol{J}(\boldsymbol{y})\, \mathrm{div}_\Gamma \boldsymbol{J}'(\boldsymbol{x})\, d\gamma_y d\gamma_x}_{a_2(\boldsymbol{J},\boldsymbol{J}')}$$

The weak form (2) is **well-posed** aside from the internal resonant frequencies[2].

1. Jean-Claude Nédélec. *Acoustic and electromagnetic equations: integral representations for harmonic problems*. Springer Science & Business Media, 2001
2. Annalisa Buffa and Ralf Hiptmair. "Galerkin boundary element methods for electromagnetic scattering". In: *Topics in computational wave propagation*. Springer, 2003, pp. 83–124

**Discretization of the EFIE problem**

Let $\mathcal{T}_h$ be a partition of $\Gamma$ into non overlapping triangular elements, $K$, s.t.

$$\bar{\Gamma} = \bigcup_{K \in \mathcal{T}_h} \bar{K},$$

We shall build the discrete EFIE problem in the following form

Find $\boldsymbol{J}_h \in \mathcal{V}_h$, such that :

$$a_h\left(\boldsymbol{J}_h, \boldsymbol{J}'_h\right) = \frac{\iota}{\kappa} \int_\Gamma \boldsymbol{E}^I_h \cdot \boldsymbol{J}'_h d\gamma_x, \quad \forall \boldsymbol{J}'_h \in \mathcal{V}_h, \tag{3}$$

where

- $\mathcal{V}_h \subset H_{div}(\Gamma)$ is the finite dimensional space of Raviart-Thomas ($\mathcal{RT}$) type[3],
- $a_h(\cdot,\cdot)$: $\mathcal{V}_h \times \mathcal{V}_h \to \mathbb{C}$ is the discrete bilinear form approximating the continuous form $a(\cdot,\cdot)$,
- the r.h.s term is an approximation of the continuouos one.

The discrete weak form (3) is **well-posed**[4].

3. Pierre-Arnaud Raviart and Jean-Marie Thomas. "A mixed finite element method for 2-nd order elliptic problems". In: *Mathematical aspects of finite element methods*. Springer, 1977, pp. 292–315
4. Annalisa Buffa and Ralf Hiptmair. "Galerkin boundary element methods for electromagnetic scattering". In: *Topics in computational wave propagation*. Springer, 2003, pp. 83–124

**Everything depends on the points of view**.

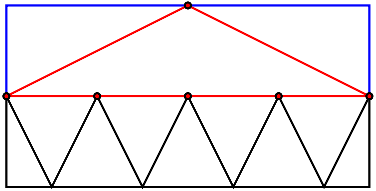

- VEM is a sort of generalization of classical FEM to polygonal/polyhedral meshes, inspired by the mimetic methods[5],
- it is a conforming Galerkin method on very general meshes, being robust wrt. element distorsion and hanging nodes.

State of the art :

**VEM framework** is applied, e.g., to

- (quasi) linear elliptic problems [Beirão da Veiga, *et al.*, 2013, 2016], [Beirão da Veiga & Manzini, 2013], [Ahmad *et al.*, 2013], [Ayuso de Dios *et al.*, 2016], [Brenner *et al.*, 2017], [Cangiani *et al.*, 2017, 2018], [Sutton, 2017], [...];
- Navier-Stokes problems [Beirão da Veiga*et al.*, 2017, 2018, 2019], [...];
- electromagnetic problems (magnetostatics, transient Maxwell eq.s, MHD,) [Brezzi & Marini, 2014], [Beirão da Veiga*et al.*, 2016, 2017, 2018, 2021];

Some other **polytopal methods**

- HDG [Cockburn],
- HHO [Ern, Di Pietro],
- ...

5. L Beirão da Veiga et al. "Basic principles of virtual element methods". In: *Mathematical Models and Methods in Applied Sciences* 23.01 (2013), pp. 199–214

**Everything depends on the points of view.**

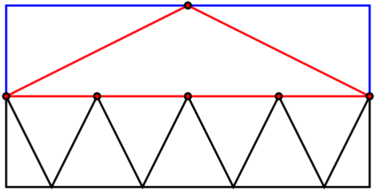

- VEM is a sort of generalization of classical FEM to polygonal/polyhedral meshes, inspired by the mimetic methods[5],
- it is a conforming Galerkin method on very general meshes, being robust wrt. element distorsion and hanging nodes.

Main ingredients of VEM :

⇒ the finite dimensional virtual space, on each element = non polynomial basis functions that are local solutions of a PDE and never explicitly computed (that's why the naming "virtual"!),

⇒ some local polynomial projection operators, computed only via the related degrees of freedom (d.o.f), that get information on basis functions.

↪ Assembly of the global linear system!

5. L Beirão da Veiga et al. "Basic principles of virtual element methods". In: *Mathematical Models and Methods in Applied Sciences* 23.01 (2013), pp. 199–214

Let $K$ be a polygon, we consider an example of construction of the virtual space $\mathcal{V}_h$ allowing :

- to guarantee the $H_{div}$ conformity and
- to ensure the accuracy of (lowest order)$\mathcal{RT}_0$-like space.

Let $K$ be a polygon, we consider an example of construction of the virtual space $\mathcal{V}_h$ allowing :

- to guarantee the $H_{div}$ conformity and
- to ensure the accuracy of (lowest order)$\mathcal{RT}_0$-like space.

The serendipity edge VEM space $\widetilde{\mathcal{V}}_h$ is defined element-wise[6]: for all $K \in \mathcal{T}_h$

$$\mathcal{V}_0^e(K) = \Big\{ \boldsymbol{v} : K \to \mathbb{C}^2 | \quad \forall e \in \partial K, (\boldsymbol{v} \cdot \boldsymbol{\nu}_e)|_e \in \mathbb{P}_0(e), \mathrm{div}\boldsymbol{v} \in \mathbb{P}_0(K)$$

$$\mathrm{rot}\boldsymbol{v} \in \mathbb{P}_0(K), \int_K \boldsymbol{v} \cdot \boldsymbol{x}_K^{\perp} dK = 0 \Big\},$$

the assembly of which builds

$$\widetilde{\mathcal{V}}_h(\mathcal{T}_h) = \left\{ \boldsymbol{v} \in H_{div}(\Gamma) | \quad \boldsymbol{v}^{\mathrm{2D}}|_K \in \mathcal{V}_0^e(K), \quad \forall K \in \mathcal{T}_h \right\},$$

where $\boldsymbol{v}^{\mathrm{2D}}|_K = \boldsymbol{v}|_K$ in local tangential coordinate system, $\boldsymbol{x}_K = \boldsymbol{x} - \boldsymbol{x}_G \in \mathbb{R}^2$, with $\boldsymbol{x}_G =$ barycenter of $K$ and $\boldsymbol{\nu}_e =$ outward unit normal to $e$.

- It holds $\mathcal{RT}_0(K) = \left\{ (\mathbb{P}_0(K))^2 \oplus \boldsymbol{x}_K \mathbb{P}_0(K) \right\} \subset \mathcal{V}_0^e(K)$, and $dim(\mathcal{V}_0^e(K)) = \sharp$ edges of $K$,
- the associated d.o.f are: for each edge $e \in \partial K$, $\boldsymbol{v} \mapsto \Lambda_e(\boldsymbol{v}) := \int_e (\boldsymbol{v} \cdot \boldsymbol{\nu}_e)|_e p_0 d\gamma, \quad \forall p_0 \in \mathbb{P}_0(e)$,
- the basis functions are $\boldsymbol{\varphi}_e$, defined by $\Lambda_{\tilde{e}}(\boldsymbol{\varphi}_e) = \delta_{e,\tilde{e}}, \quad \forall e, \tilde{e} \in \partial K$ (solution of a local PDE), but, a priori, they are no longer polynomials. They are unknowns (never computed) inside $K$!

6. L Beirão da Veiga et al. "Lowest order virtual element approximation of magnetostatic problems". In: *Computer Methods in Applied Mechanics and Engineering* 332 (2018), pp. 343–362

Remark: via the only knowledge of d.o.f, it is possible to compute, $\forall \boldsymbol{v} \in \mathcal{V}_0^e(K)$

⇒ the constant value of $\mathrm{div}\boldsymbol{v}$ on $K$, as : $\mathrm{div}\boldsymbol{v} = \frac{1}{|K|}\int_K \mathrm{div}\boldsymbol{v} dK = \int_{\partial K} (\boldsymbol{v}\cdot\boldsymbol{\nu}_e)|_{\partial K} ds$,

⇒ the $L^2$-orthogonal projection operator, $\Pi_0^{K,s}$, of basis functions onto $(\mathbb{P}_s(K))^2$, with $s \leq 1$. Particularly,

$$\Pi_0^{K,1} : \mathcal{V}_0^e(K) \to (\mathbb{P}_1(K))^2 = \mathbf{grad}\mathbb{P}_2(K) \oplus \boldsymbol{x}_K^{\perp}\mathbb{P}_0(K), \text{ defined by } :\forall \boldsymbol{p}_1 \in (\mathbb{P}_1(K))^2$$

$$\begin{aligned}
\int_K \Pi_0^{K,1}\boldsymbol{v}\cdot\boldsymbol{p} dK &= \int_K \boldsymbol{v}\cdot\boldsymbol{p} dK \\
&= \int_K \boldsymbol{v}\cdot\left(\mathbf{grad} p_2 + \boldsymbol{x}_K^{\perp} p_0\right) dK \\
&= -\underbrace{\int_K \mathrm{div}\boldsymbol{v} p_2 dK}_{\text{Computable!}} + \underbrace{\int_{\partial K} (\boldsymbol{v}\cdot\boldsymbol{\nu})_{|\partial K}\, p_2 ds}_{\text{Computable!}} + \underbrace{\int_K \boldsymbol{v}\cdot\boldsymbol{x}_K^{\perp} p_0 dK}_{=0}.
\end{aligned}$$

- it holds $\Pi_0^{K,1}\boldsymbol{q} = \boldsymbol{q}, \quad \forall \boldsymbol{q} \in \mathcal{RT}_0(K)$,
- if $K$ = triangle, then $\mathcal{V}_0^e(K) = \mathcal{RT}_0(K)$, otherwise $\mathcal{RT}_0(K) \subset \mathcal{V}_0^e(K)$.

The real face of virtual basis functions.

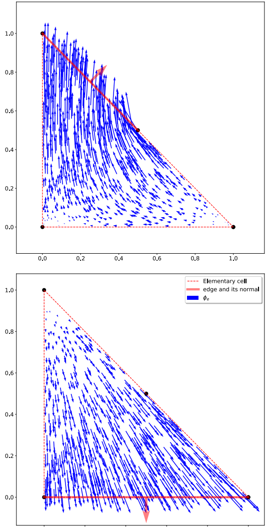


Figure: Non-serendipity virtual basis functions.

Their $L^2$-projection onto $(\mathbb{P}_1(K))^2$.

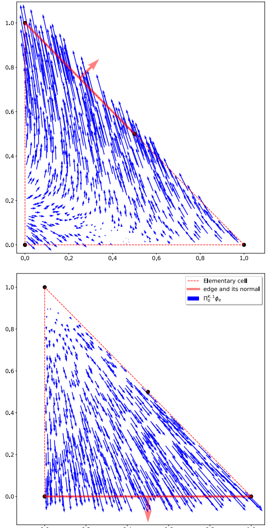


Figure: Projection of virtual basis functions.

Recalling the discrete EFIE problem: Find $\boldsymbol{J}_h \in \widetilde{\mathcal{V}}_h$, such that :

$$a_h\left(\boldsymbol{J}_h, \boldsymbol{J}_h'\right) = \frac{\iota}{\kappa}\int_\Gamma \boldsymbol{E}_h^I \cdot \boldsymbol{J}_h' d\gamma_x, \quad \forall \boldsymbol{J}_h' \in \widetilde{\mathcal{V}}_h,$$

- $a_h(\cdot,\cdot)$ is built element-wise

$$a_h\left(\boldsymbol{J}_h, \boldsymbol{J}_h'\right) = \sum_{K\in\mathcal{T}_h}\sum_{L\in\mathcal{T}_h} a_h^{K,L}\left(\boldsymbol{J}_h, \boldsymbol{J}_h'\right), \quad \forall \boldsymbol{J}_h, \boldsymbol{J}_h' \in \widetilde{\mathcal{V}}_h,$$

where $a_h^{K,L}(\cdot,\cdot)$ is the local bilinear form on $\widetilde{\mathcal{V}}_{h|_K} \times \widetilde{\mathcal{V}}_{h|_L}$, that, via the basis functions reads as

$$a_h^{K,L}\left(\boldsymbol{\varphi}_i, \boldsymbol{\varphi}_j'\right) = \underbrace{\mu \int_{K\times L} G_\kappa(\boldsymbol{x}-\boldsymbol{y})\,\Pi_0^{K,1}\boldsymbol{\varphi}_i \cdot \Pi_0^{L,1}\boldsymbol{\varphi}_j' d\gamma_y d\gamma_x}_{a_{h,1}^{K,L}(\boldsymbol{\varphi}_i,\boldsymbol{\varphi}_j')} - \underbrace{\frac{1}{\kappa^2\varepsilon}\int_{K\times L} G_\kappa(\boldsymbol{x}-\boldsymbol{y})\,\mathrm{div}_\Gamma\boldsymbol{\varphi}_i \mathrm{div}_\Gamma\boldsymbol{\varphi}_j' d\gamma_y d\gamma_x}_{a_{h,2}^{K,L}(\boldsymbol{\varphi}_i,\boldsymbol{\varphi}_j')}.$$

$\forall$ edges $i\in\partial K$
$\forall$ edges $j\in\partial L$

- As for the discrete r.h.s term, let $\boldsymbol{E}_h^I = \Pi_0^{K,1}\boldsymbol{E}^I$ on each $K \in \mathcal{T}_h$, we have

$$\int_\Gamma \boldsymbol{E}_h^I \cdot \boldsymbol{J}_h' d\gamma = \sum_{K\in\mathcal{T}_h}\int_K \boldsymbol{E}^I\,\Pi_0^{K,1}\boldsymbol{J}_h' d\gamma_x, \quad \forall \boldsymbol{J}_h' \in \widetilde{\mathcal{V}}_h.$$

- Solution of the global linear system via a direct numerical method.

- In the standard VEM framework, the projector is linked with an operator to be discretized:
  - $\Pi_0^{K,1}$ for mass matrix (or $H^1$-type projector for stiffness term),
  - which allows the construction of the local $L^2$ scalar product as, $\forall$ VEM functions:

$$(u, v)_{0,K} \approx \left(\Pi_0^{K,1} u, \Pi_0^{K,1} v\right)_{0,K} + \underbrace{S_K\left(\left(\mathbf{I} - \Pi_0^{K,1}\right) u, \left(\mathbf{I} - \Pi_0^{K,1}\right) v\right)}_{\substack{\text{stabilization term scaling like the} \\ L^2 \text{ norm on VEM fct.s}}}.$$

- A similar approach is not possible for integral equations due to the non-local nature of the operators: the projection r.h.s term can not be only computed from d.o.f..
- The "sub-principal" term within the EFIE is (roughly) approximated by using a $L^2$-projection of the virtual basis functions.
- **Work to be done**: uniform inf-sup condition of the discrete bilinear form.

## Some preliminary numerical results

## Simulation of the EM scattering of a plane wave by a perfectly conducting sphere.

**Data** :

- wave frequency $f = 0.5GHz$ ($\lambda \approx 0.6m$),
- sphere radius $R \approx 1.66\lambda$,
- plane wave incoming from the sphere top (yellow side),
- partition of $\Gamma$ with a family of
  - conforming meshes, and
  - regular nonconforming meshes of triangle-shape elements,
- exact solution for $J$ and RCS available.

**Aim of this study**:

1. convergence rate with mesh of $L^2$-error
   - on $\boldsymbol{J}$ as
   $$\frac{\left\|\boldsymbol{J} - \Pi_0^1 \boldsymbol{J}_h\right\|_{0,\Gamma}}{\|\boldsymbol{J}\|_{0,\Gamma}},$$
   - and on $\mathrm{div}\boldsymbol{J}$ as
   $$\frac{\|\mathrm{div}\,(\boldsymbol{J} - \boldsymbol{J}_h)\|_{0,\Gamma}}{\|\mathrm{div}\boldsymbol{J}\|_{0,\Gamma}}.$$
2. bistatic RCS and distribution of $\boldsymbol{J}_h$ on the sphere.

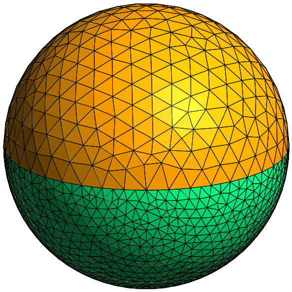

Figure: Nonconforming mesh of the sphere boundary.

$L^2$-error on $\boldsymbol{J}$ (deep) and on $\mathrm{div}\boldsymbol{J}$ (light) obtained from classical $\mathcal{RT}$-like and VEM-like methods.

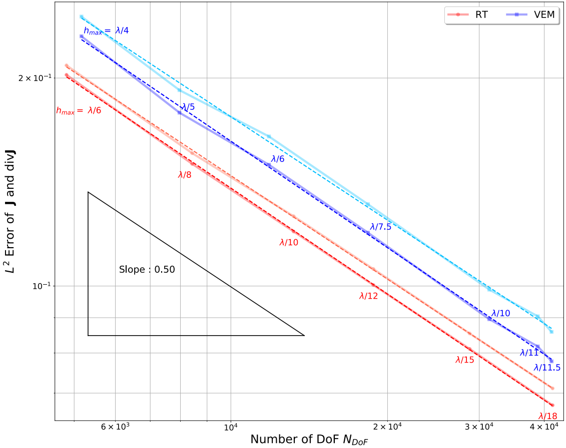

$\mathcal{RT}$-like method vs. VEM-like method (exact solution)

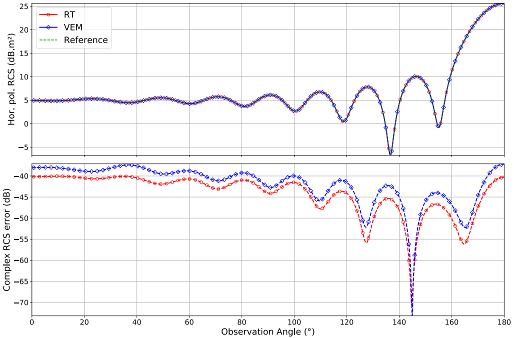


Figure: H-polarized bistatic RCS (top) and its complex errors (bottom).

Current distribution on the sphere.

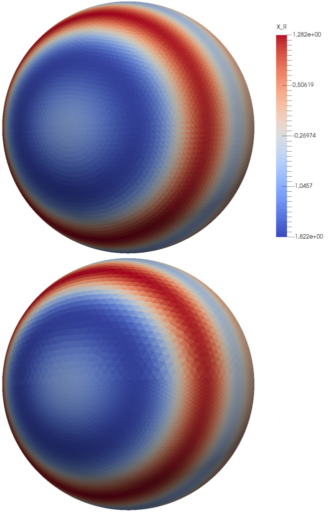


Figure: Real part of the $x$-component of $\boldsymbol{J}_h$ from $\mathcal{RT}$-like (top) and VEM-like (bottom) methods.

## Simulation of the EM scattering of a plane wave by a perfectly conducting cone.

**Data** :

- Wave frequency $f = 5GHz$ ($\lambda \approx 0.06m$),
- cone size $\approx 1.66\lambda \times 8.33\lambda$,
- plane wave incoming from the cone apex,
- partition of $\Gamma$ with
  - a conforming mesh with mean size $h = \lambda/10$, and
  - an arbitrary nonconforming mesh with fine-coarse ratio $1 : 5$.

**Aim of this study**:

1 the bistatic RCS from a nonconforming mesh of the cone.

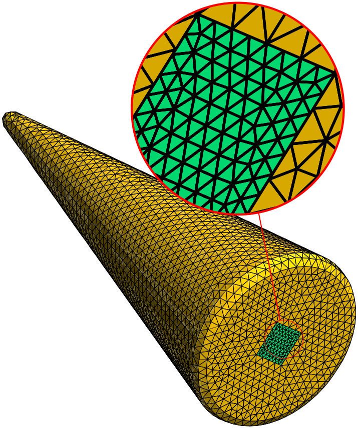

Figure: Nonconforming mesh of the cone base.

$\mathcal{RT}$-like method vs. VEM-like method

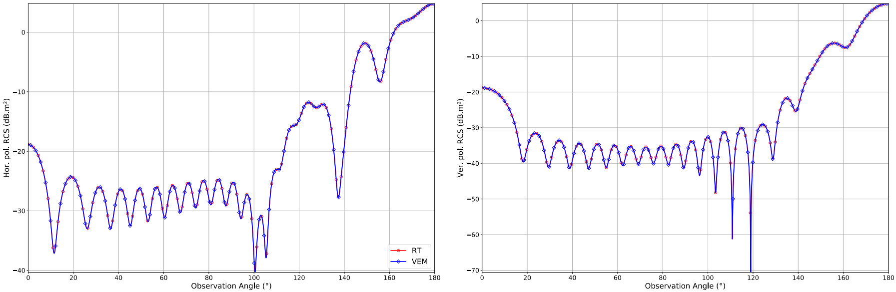


Figure: H- (left) and V-polarized (right) bistatic RCS.

# Conclusion

Summary :

- First reflection on the application of VEM to the Maxwell boundary integral equation of EFIE type,
- Promising preliminary numerical results.

Outlook (within the ongoing PhD thesis of Alexis Touzalin, 2022-2025) :

- theoretical and numerical analysis of math. properties of the VEM scheme, (e.g. well-posedness, matrix conditioning, etc.),
- study of more suitable VEM-like projection operators,
- application of VEM to other Maxwell boundary integral formulations and various test cases with increasing complexity (e.g. meshes on curved interfaces/boundaries).

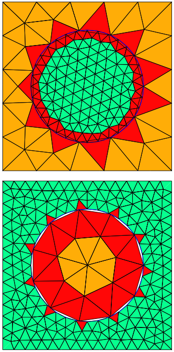

Figure: Nonconforming meshes of curved interfaces.

**Thank you for your attention!**

www.cea.fr

**Annex**

Thanks to the polynomial nature of virtual projections, the singular integrals within $a_h(\cdot,\cdot)$, due to the Green kernel, are treated by

1. partitioning each polygon $K$ into sub-triangles and
2. applying a numerical singularity extraction technique[7] triangle-wise.

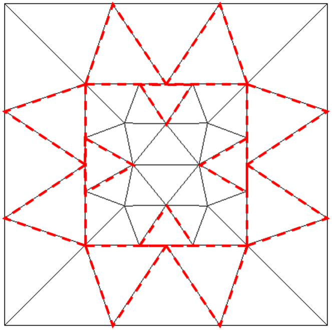

Figure: Example of nonconforming mesh.

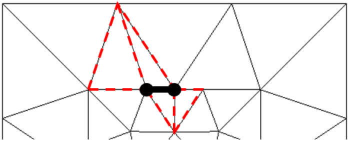

Figure: Example of edge extraction.

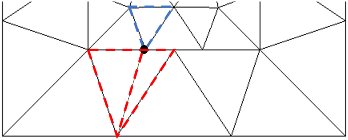

Figure: Example of single-point extraction.

7. Eric Darrigrand. "Couplage Methodes Multipoles - Discretisation Microlocale pour les Equations Integrales de l'Electromagnetisme". Theses. Université Sciences et Technologies - Bordeaux I, Sept. 2002

The Raviart-Thomas space of lowest order can be defined as follows:

$$\mathcal{V}_h(\mathcal{T}_h) = \left\{ \boldsymbol{v} \in H_{div}(\Gamma) \mid \quad \boldsymbol{v}^{2\mathrm{D}}|_K \in \mathcal{RT}_0(K), \quad \forall K \in \mathcal{T}_h \right\},$$

where $\boldsymbol{v}^{2\mathrm{D}}|_K = \boldsymbol{v}|_K$ in local tangential coordinate system,

$$\mathcal{RT}_0(K) := \left\{ \boldsymbol{v} \in (\mathbb{P}_0(K))^2 \oplus \boldsymbol{x}_K \mathbb{P}_0(K) \mid \quad (\boldsymbol{v}\cdot\boldsymbol{\nu}_e)|_{\partial K} \in L^2(\partial K), (\boldsymbol{v}\cdot\boldsymbol{\nu}_e)|_e \in \mathbb{P}_0(e), \forall \text{ edges } e \in \partial K \right\},$$

and $\boldsymbol{x}_K = \boldsymbol{x} - \boldsymbol{x}_G \in \mathbb{R}^2$, with $\boldsymbol{x}_G$ = barycenter of $K$ and $\boldsymbol{\nu}_e$ = outward unit normal to $e$.

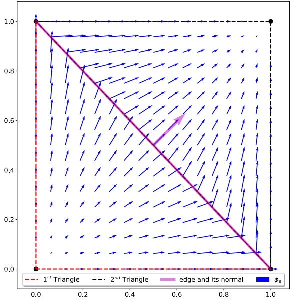


Figure: The $\mathcal{RT}_0$-like basis functions on elementary triangles.

- $dim(\mathcal{RT}_0(K)) = 3$,
- the associated degrees of freedom (d.o.f) are: for each edge $e \in \partial K$,

$$\boldsymbol{v} \mapsto \Lambda_e(\boldsymbol{v}) := \int_e (\boldsymbol{v}\cdot\boldsymbol{\nu}_e)|_e p_0 \, d\gamma, \quad \forall p_0 \in \mathbb{P}_0(e).$$

- the basis functions spanning the space $\mathcal{V}_h$ are: $\boldsymbol{\varphi}_e$

$$\Lambda_{\tilde{e}}(\boldsymbol{\varphi}_e) = \delta_{e,\tilde{e}}; \quad \forall e, \tilde{e} \in \partial K,$$

and, particularly, $\mathrm{div}\boldsymbol{\varphi}_e = \frac{1}{|K|}$, so that :

$$\boldsymbol{v}_h = \sum_{e\in\partial K} \Lambda_e(\boldsymbol{v}_h)\boldsymbol{\varphi}_e, \quad \forall \boldsymbol{v}_h \in \mathcal{RT}_0(K).$$

The Raviart-Thomas space of lowest order can be defined as follows:

$$\mathcal{V}_h(\mathcal{T}_h) = \left\{ \boldsymbol{v} \in H_{div}(\Gamma) \mid \quad \boldsymbol{v}^{2\mathrm{D}}|_K \in \mathcal{RT}_0(K), \quad \forall K \in \mathcal{T}_h \right\},$$

where $\boldsymbol{v}^{2\mathrm{D}}|_K = \boldsymbol{v}|_K$ in local tangential coordinate system,

$$\mathcal{RT}_0(K) := \left\{ \boldsymbol{v} \in (\mathbb{P}_0(K))^2 \oplus \boldsymbol{x}_K \mathbb{P}_0(K) \mid \quad (\boldsymbol{v} \cdot \boldsymbol{\nu}_e)|_{\partial K} \in L^2(\partial K), (\boldsymbol{v} \cdot \boldsymbol{\nu}_e)|_e \in \mathbb{P}_0(e), \forall \text{ edges } e \in \partial K \right\},$$

and $\boldsymbol{x}_K = \boldsymbol{x} - \boldsymbol{x}_G \in \mathbb{R}^2$, with $\boldsymbol{x}_G$ = barycenter of $K$ and $\boldsymbol{\nu}_e$ = outward unit normal to $e$.

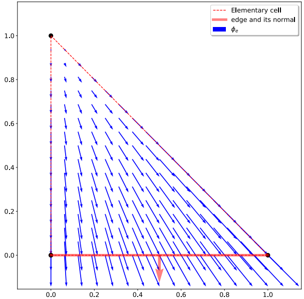


Figure: The $\mathcal{RT}_0$-like basis functions on elementary triangle.

- $dim(\mathcal{RT}_0(K)) = 3$,
- the associated degrees of freedom (d.o.f) are: for each edge $e \in \partial K$,

$$\boldsymbol{v} \mapsto \Lambda_e(\boldsymbol{v}) := \int_e (\boldsymbol{v} \cdot \boldsymbol{\nu}_e)|_e p_0 \, d\gamma, \quad \forall p_0 \in \mathbb{P}_0(e).$$

- the basis functions spanning the space $\mathcal{V}_h$ are: $\boldsymbol{\varphi}_e$

$$\Lambda_{\tilde{e}}(\boldsymbol{\varphi}_e) = \delta_{e,\tilde{e}}; \quad \forall e, \tilde{e} \in \partial K,$$

and, particularly, $\mathrm{div}\boldsymbol{\varphi}_e = \frac{1}{|K|}$, so that :

$$\boldsymbol{v}_h = \sum_{e \in \partial K} \Lambda_e(\boldsymbol{v}_h) \boldsymbol{\varphi}_e, \quad \forall \boldsymbol{v}_h \in \mathcal{RT}_0(K).$$

The Raviart-Thomas space of lowest order can be defined as follows:

$$\mathcal{V}_h(\mathcal{T}_h) = \left\{ \boldsymbol{v} \in H_{div}(\Gamma) \mid \quad \boldsymbol{v}^{\mathrm{2D}}|_K \in \mathcal{RT}_0(K), \quad \forall K \in \mathcal{T}_h \right\},$$

where $\boldsymbol{v}^{\mathrm{2D}}|_K = \boldsymbol{v}|_K$ in local tangential coordinate system,

$$\mathcal{RT}_0(K) := \left\{ \boldsymbol{v} \in (\mathbb{P}_0(K))^2 \oplus \boldsymbol{x}_K \mathbb{P}_0(K) \mid \quad (\boldsymbol{v}\cdot\boldsymbol{\nu}_e)|_{\partial K} \in L^2(\partial K), (\boldsymbol{v}\cdot\boldsymbol{\nu}_e)|_e \in \mathbb{P}_0(e), \forall \text{ edges } e \in \partial K \right\},$$

and $\boldsymbol{x}_K = \boldsymbol{x} - \boldsymbol{x}_G \in \mathbb{R}^2$, with $\boldsymbol{x}_G$ = barycenter of $K$ and $\boldsymbol{\nu}_e$ = outward unit normal to $e$.

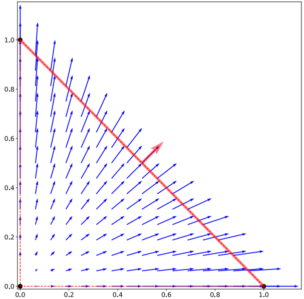


Figure: The $\mathcal{RT}_0$-like basis functions on elementary triangle.

- $dim(\mathcal{RT}_0(K)) = 3$,
- the associated degrees of freedom (d.o.f) are: for each edge $e \in \partial K$,

$$\boldsymbol{v} \mapsto \Lambda_e(\boldsymbol{v}) := \int_e (\boldsymbol{v}\cdot\boldsymbol{\nu}_e)|_e p_0 \, d\gamma, \quad \forall p_0 \in \mathbb{P}_0(e).$$

- the basis functions spanning the space $\mathcal{V}_h$ are: $\boldsymbol{\varphi}_e$

$$\Lambda_{\tilde{e}}(\boldsymbol{\varphi}_e) = \delta_{e,\tilde{e}}; \quad \forall e, \tilde{e} \in \partial K,$$

and, particularly, $\mathrm{div}\boldsymbol{\varphi}_e = \frac{1}{|K|}$, so that :

$$\boldsymbol{v}_h = \sum_{e\in\partial K} \Lambda_e(\boldsymbol{v}_h)\,\boldsymbol{\varphi}_e, \quad \forall \boldsymbol{v}_h \in \mathcal{RT}_0(K).$$

The Raviart-Thomas space of lowest order can be defined as follows:

$$\mathcal{V}_h(\mathcal{T}_h) = \left\{ \boldsymbol{v} \in H_{div}(\Gamma) \mid \quad \boldsymbol{v}^{2\mathrm{D}}|_K \in \mathcal{RT}_0(K), \quad \forall K \in \mathcal{T}_h \right\},$$

where $\boldsymbol{v}^{2\mathrm{D}}|_K = \boldsymbol{v}|_K$ in local tangential coordinate system,

$$\mathcal{RT}_0(K) := \left\{ \boldsymbol{v} \in (\mathbb{P}_0(K))^2 \oplus \boldsymbol{x}_K \mathbb{P}_0(K) \mid \quad (\boldsymbol{v} \cdot \boldsymbol{\nu}_e)|_{\partial K} \in L^2(\partial K), (\boldsymbol{v} \cdot \boldsymbol{\nu}_e)|_e \in \mathbb{P}_0(e), \forall \text{ edges } e \in \partial K \right\},$$

and $\boldsymbol{x}_K = \boldsymbol{x} - \boldsymbol{x}_G \in \mathbb{R}^2$, with $\boldsymbol{x}_G$ = barycenter of $K$ and $\boldsymbol{\nu}_e$ = outward unit normal to $e$.

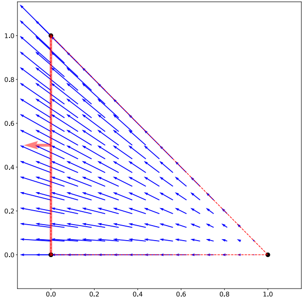


Figure: The $\mathcal{RT}_0$-like basis functions on elementary triangle.

- $dim(\mathcal{RT}_0(K)) = 3$,
- the associated degrees of freedom (d.o.f) are: for each edge $e \in \partial K$,

$$\boldsymbol{v} \mapsto \Lambda_e(\boldsymbol{v}) := \int_e (\boldsymbol{v} \cdot \boldsymbol{\nu}_e)|_e p_0 \, d\gamma, \quad \forall p_0 \in \mathbb{P}_0(e).$$

- the basis functions spanning the space $\mathcal{V}_h$ are: $\boldsymbol{\varphi}_e$

$$\Lambda_{\tilde{e}}(\boldsymbol{\varphi}_e) = \delta_{e,\tilde{e}}; \quad \forall e, \tilde{e} \in \partial K,$$

and, particularly, $\mathrm{div}\boldsymbol{\varphi}_e = \frac{1}{|K|}$, so that :

$$\boldsymbol{v}_h = \sum_{e \in \partial K} \Lambda_e(\boldsymbol{v}_h) \boldsymbol{\varphi}_e, \quad \forall \boldsymbol{v}_h \in \mathcal{RT}_0(K).$$